Pressure Drop in a Split-and-Recombine Caterpillar Micromixer in Case of Newtonian and Non-Newtonian Fluids

Odile Carrier, Denis Funfschilling, Hélène Debas, and Souhila Poncin
Laboratoire Réactions et Génie des Procédés (LRGP), Université de Lorraine, CNRS, Nancy F-54001, France

Patrick Löb
Institut für Mikrotechnik Mainz GmbH, Mainz D-55129, Germany

Huai-Zhi Li
Laboratoire Réactions et Génie des Procédés (LRGP), Université de Lorraine, CNRS, Nancy F-54001, France

DOI 10.1002/aic.14035
Published online February 22, 2013 in Wiley Online Library (wileyonlinelibrary.com)

Microreactors are very promising tools for the design of future chemical processes. For example, emulsions of very narrow size distribution are obtained at much lower energy consumption than the one spent with usual processes. Micromixers play thereby an eminent role. The goal of this study is to better understand the hydrodynamic properties of a split-and-recombine Caterpillar micromixer (CPMM) specially with regard to handling viscoelastic fluids, a topic hardly addressed so far in the context of micromixers in general, although industrial fluids like detergent, cosmetic, or food emulsions are non-Newtonian. Friction factor was measured in a CPMM for both Newtonian and non-Newtonian fluids. For Newtonian fluids, the friction factor in the laminar regime is $f/2 = 24/Re$. The laminar regime exists up to Reynolds numbers of 15. For shear-thinning fluids like Carbopol 940 or viscoelastic fluids like Poly Acryl Amide (PAAm) aqueous solutions, the friction factor scales identically within statistical errors up to a generalized Reynolds number of 10 and 0.01, respectively. Above that limit, there is an excess pressure drop for the viscoelastic PAAm solution. This excess pressure drop multiplies the friction factor by more than a decade over a decade of Reynolds numbers. The origin of this excess pressure drop is the high elongational flow present in the Caterpillar static mixer applied to a highly viscoelastic fluid. This result can be extended to almost all static mixers, because their flows are generally highly elongational. © 2013 American Institute of Chemical Engineers *AIChE J*, 59: 2679–2685, 2013

Keywords: non-Newtonian fluid, viscoelasticity, elongational flow, micromixer, caterpillar, pressure drop, excess pressure drop, friction factor

Introduction

Microreactors are very promising tools for process intensification and green and safe chemistry.[1–7] Micromixers have at least three important features that make them particularly interesting for chemical synthesis[1,8]: (1) they have an excellent heat-transfer capability due to their high surface to volume ratio that enables an excellent control of the temperature. It is very useful for highly endothermic or exothermic reactions. This excellent heat transfer also prevents the formation of potentially dangerous hot spots. It opens up new fields of chemical synthesis and reactions; (2) in micromixers and microreactors, residence times are very easy to control and can be made very short; (3) moreover, the mixing time can be short and quality of the mixing is usually excellent. Good control of the residence time and mixing quality are essential for the control of the kinetics of reactions, which is the key for an enhanced selectivity and yield. Besides that, this control makes it possible to handle reactions in the explosive regime or reactions with fast decomposing reactants.[5] Hence, microreactors allow working under process conditions nonapplicable with conventional equipment, that is, microreactors open Novel Process Windows.[3]

Micromixers play an eminent role in all this. They are part of the larger family of static mixers who have been intensively studied in the last two decades not only due to their excellent performance in the field of mixing and two phase dispersion but also in their ability to redesign a discontinuous process into a continuous process.[9–14] Most of the studies on static mixer were focused on experimental measurements of pressure loss, heat transfer, and mixing. Numerical simulations were also performed on such systems.[11,14] In the later article, it was observed that a shear-thinning viscosity improve mixing quality, mixing efficiency, and lower the pressure drop in SMX static mixer compare with Newtonian fluids.

It is only in recent years that micron-size mixers have been technically largely available thanks to the emergence of research centers and commercial suppliers dedicated to microfabrication and able to manufacture high-precision micromixers in variety of materials.

There is an almost unmanageable variety of micromixers described and available in the meantime (see Ref. 15 for a

Correspondence concerning this article should be addressed to D. Funfschilling at denis.funfschilling@univ-lorraine.fr.

review). Most of them rely on multilamination initiated by interdigital lamella arrangement, on chaotic mixing or on a successive split-and-recombine (SAR) approach (Refs. 16 and references given therein and 17). The focus of this article is on the so-called Caterpillar micromixer (CPMM) type from IMM (Institut für Mikrotechnik Mainz GmbH, Mainz, Germany), which follows essentially the SAR principle. In an ideal SAR mixer, the stream is divided into two substreams in each element of the mixer, and these two substreams are folded/guided over each other and recombined in horizontal and vertical planes. By repeated application, one ends up in a multilaminated flow and an exponentially increased interfacial area between the different elements of the stream. So, when starting with a two lamella configuration of 1200 × 1200 μm^2 cross section, after eight mixing steps, the fluid is ideally divided into 512 lamellae of 2.4 μm width. Schönfeld et al.[16] pointed out that albeit having a highly regular flow pattern in this ideal SAR mixers, mixing is characterized by a positive finite-time Lyapunov exponent, which shows chaotic advection that proves an improved mixing efficiency.

Albeit the CPMM type considered in this work follows in its design the SAR approach, the principle is only imperfectly realized[16]: for example, at low *Re*, the initial lamination is not kept due to internal friction, and at higher *Re*, inertial forces induce a secondary flow that lead finally to a considerable increase of interfacial area—both lead to a loss of the ideal regular multilaminated flow. CPMMs have been used in several synthesis.[4,6,18,19] They also reduce the energy needed to mix or to disperse gas or liquids.[2,4,20]

Despite the growing interest in micromixers for industrial applications as well as research tools, their flow characteristics are still far from being completely known. Working with micron-size micromixers (the Caterpillar has almost micron size, 1200 μm) changes the balance between volume forces (like inertia and gravity) and surface forces (like shear stresses or surface tension) in favor of the latest. This change of scale is one originality of this work. The goal of this work is to characterize a CPMM (in the following called only Caterpillar) in terms of pressure drop for Newtonian and shear thinning—viscoelastic fluids.

The pressure drop is measured in a SAR CPMM for Newtonian and non-Newtonian fluids. From the rheological properties of the fluids, we will be able to calculate the pressure drop and shear rate[10–14] inside the Caterpillar in case of emulsification processes. This article is organized as follows: in the first section, the experimental set-up and fluids properties are presented. Then, the pressure drop is measured in the case of Newtonian fluids. A Metzner–Otto like constant is measured to establish a correlation predicting the pressure drop in the Caterpillar, knowing the rheological characteristics of the fluids. The last section of this article is devoted to the excess pressure drop that is observed in the case of viscoelastic fluids.

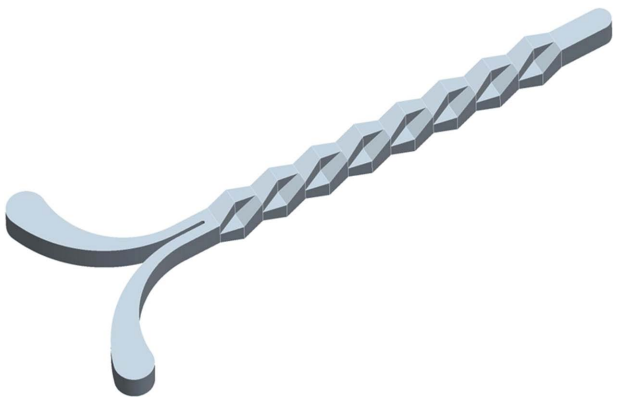

Figure 1. Technical sketch of the CPMM internal structure.

Visible is the ramp-like structure of the central mixing channel. [Color figure can be viewed in the online issue, which is available at wileyonlinelibrary.com.]

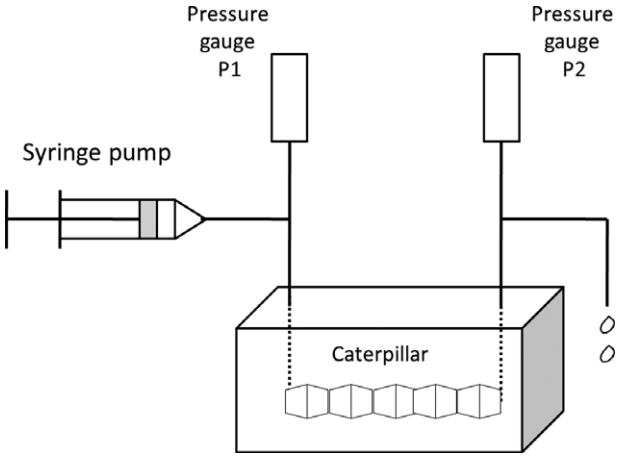

Figure 2. Experimental set-up.

Experiments

Experimental set-up for pressure drop measurements

The Caterpillar used is a CPMM-V1.2-R1200/8 (Caterpillar Micro Mixer R1200/8) from IMM. The cross section of the Caterpillar is quite complex due to its shape that drives the SAR mixing. However, the Caterpillar channel is more or less inscribed in 1200 × 1200 μm^2 cross-section. Hence, $d = 1200$ μm can be considered as the characteristic dimension of the Caterpillar. The Caterpillar consists of eight mixing elements of $l = 2400$ μm long each, so that the total length of the mixing zone is $L = 19{,}200$ μm. A technical sketch of the internal Caterpillar structure is given in Figure 1.

The experimental set-up is presented in Figure 2. The flow rate was imposed by a Harvard Apparatus PHD 2000 syringe pump (Harvard Apparatus, Holliston, MA). The pressure drop was measured by two high-precision pressure gauges (PR234/0.5 bar and PR-41X/0.1 bar, precision: 0.08% of full scale, Keller, Druckmesstechnik, Germany). The pressure was acquired on a 12Bits Labjack U12 acquisition card (LabJack, Lakewood, CO). Connecting pipes were chosen as short as possible and have diameter of at least 3.5 mm to avoid additional pressure drop. The pressure drop through the Caterpillar is the pressure drop through the set-up from which the pressure drop measured when connecting directly the entrance and exit feeding pipes of the Caterpillar is subtracted.

Determination of fluid properties

Eight Newtonian (distilled water and Emkarox/water solutions), one non-Newtonian shear-thinning fluid (Carbopol 940 solution), and three non-Newtonian viscoelastic fluids

Table 1. Densities and Viscosities of Newtonian Fluids at 20°C

	Density ρ (kg/m^3)	Viscosity η (Pa. s)
Water	998	0.001
Emkarox d1007	1007	0.015
Emkarox d1019	1019	0.029
Emkarox d1020	1020	0.038
Emkarox d1046	1046	0.210
Emkarox d1060	1060	1.2
Emkarox d1067	1067	1.16
Emkarox d1082	1082	3.3

PAAm (polyacrylamide solutions) were used. The rheological properties of the different fluids are thoroughly characterized. The viscosities of Emkarox/water mixtures were measured with a capillary Ubbelohde viscosimeter (AVS 310, Schott Geräte, Germany; see Table 1). Carbopol 940 0.4% in mass aqueous solution was used as shear-thinning nonviscoelastic fluid. PAAm 0.1, 0.25, and 0.5% in mass aqueous solutions were used as viscoelastic shear-thinning fluids (AN 913 SH, SNF Floerger, 42163 Andrézieux, France). Viscosities were measured with an ARG2 (TA Instrument, New Castle, DE 19720). The shear rate dependent viscosities of the PAAm and Carbopol solutions are given in Figure 3. The viscosity of PAAm and Carbopol solutions can be modeled by a power law in the range of shear rates usually used in industrial applications

$$\eta = k\dot{\gamma}^{n-1} \tag{1}$$

where η is the dynamic viscosity, n is the flow index, $\dot{\gamma}$ the shear rate, and k the flow consistency index. A more complete representation of the viscosity is given by the Carreau law for a wide range of shear rates

$$\frac{\eta-\eta_\infty}{\eta_0-\eta_\infty} = \left[1+(\lambda\dot{\gamma})^2\right]^{\frac{m-1}{2}} \tag{2}$$

The parameters of the viscosity models for the non-Newtonian fluids are summarized in Table 2.

As the PAAm solutions are highly elastic, they have important first normal stresses that have been measured with a cone and plate geometry on an ARG2 rheometer (TA Instruments, New Castle DE 19720) and are given in Figure 3.

Elongational time scales were also measured on a polymeric filament thinning experimental set-up for the non-Newtonian fluids. The microfluidic flow-focusing geometry of Ref. 21 was used. The continuous phase was a $\mu_c = 10 \times 10^{-3}$ Pa.s silicon oil. The dispersed phases were the different PAAm solutions. PAAm droplets were formed, and the formation, thinning, and break-up of the neck are recorded on a high-speed camera (CamRecord 600, Optronis, Germany). The continuous phase is coming from the side channels, the dispersed phase from the central channel (Figure 4). All the

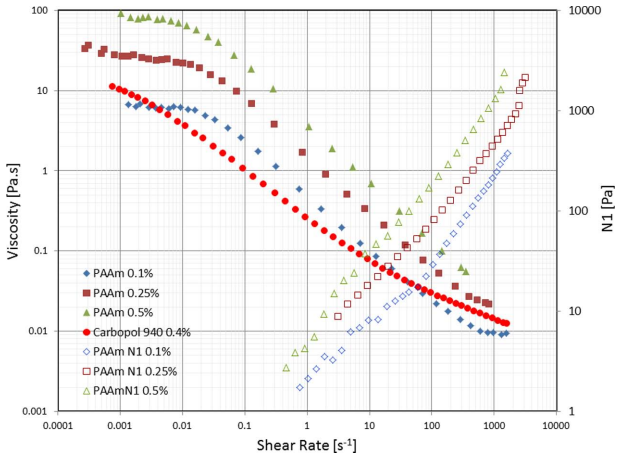

Figure 3. Viscosity and first normal stresses of the 0.4% Carbopol 940 and 0.1, 0.25, and 0.5% aqueous PAAm solutions at 20°C.

[Color figure can be viewed in the online issue, which is available at wileyonlinelibrary.com.]

channels have a square cross section and a width of 250 μm. The flow rates of the continuous phase and the dispersed phase vary from 5 to 10 μL min^{-1} and from 0.2 to 1 mL min^{-1}, respectively. A Matlab image analysis program gives the temporal evolution of the width of the neck $h(t)$. Similar to Ref. 22 two regions of exponential decay of the filament are observed (Figure 5). The extensional strain rate can be immediately deduced from the neck width as follows[22]

$$\dot{\varepsilon} = -\frac{2}{h}\frac{dh}{dt} \tag{3}$$

An elongational characteristic time can be calculated from the exponential decay of the second region by $h(t) = Ce^{-t/3\lambda_E}$.[23,24]

The characteristic elongational time λ_E (Table 3) is very similar to the one given by Bendova et al. We will see in the next section that this characteristic elongational time is of the same order of magnitude as λ_{ve}, the effective viscoelastic time characteristic of the excess pressure loss (see "Excess Pressure Drop" section).

Results and Discussion

Pressure drop in the Caterpillar is measured in the case of Newtonian fluids, shear-thinning fluids, and viscoelastic fluids. It is an important characteristic of the Caterpillar, because the product between the pressure drop and the volumetric flow rate is the energy dissipation inside the micromixer. The energy dissipation is a key parameter in many operations like in emulsification or mixing.

Table 2. Densities, Power Law Coefficients and Carreau Viscosity Law Coefficients of the Carbopol 940 and PAAm Non-Newtonian Fluids at 20°C

		Power Law		Carreau Law			
	Density (kg m^{-3})	k (Pa s^{-n})	N	η_0 (Pa s)	η_∞ (Pa s)	λ (s)	m
PAAm 0.1%	998	0.5	0.331	6.3	0.00615	38.3	0.29
PAAm 0.25%	999	1.54	0.294	25	0.009	50.6	0.28
PAAm 0.5%	1001	3.94	0.258	84	0.0016	69.5	0.27
Carbopol 940 0.4%	1000	0.32	0.499				

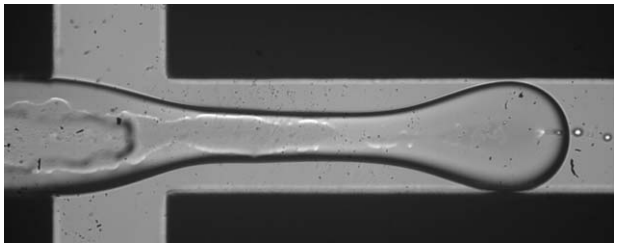

Figure 4. PAAm filament thinning in a flow-focusing geometry for a 0.25% PAAm aqueous solution.

Pressure drop for Newtonian fluids

The pressure drop through a pipe or any static mixer is characterized by a nondimensional friction factor coefficient $f/2$ defined as

$$\frac{f}{2}=\frac{\Delta P}{4\rho u^2}\frac{d}{L} \tag{4}$$

where ΔP is the pressure drop through the static mixer, ρ the density of the fluid, u the superficial velocity, d the characteristic diameter of the static mixer, and L is the total length of the micromixer. An analytical calculation shows that $f/2 = 8/Re$ for a cylindrical pipe in the laminar regime, that is, for Reynolds numbers less than 2100. The Reynolds number for Newtonian fluids is defined as

$$Re=\frac{\rho u d}{\eta} \tag{5}$$

The friction factor is measured in the Caterpillar for distilled water and for Newtonian Emkarox solutions over a large range of Reynolds numbers (Figure 6). The friction factor scales as

$$\frac{f}{2}=\frac{24\pm 1.04}{\mathrm{Re}} \tag{6}$$

up to a Reynolds number of 100 where the intermediate regime begins. It is interesting to see that this value is quite close to the range of Reynolds numbers ($Re < 15$), where an almost ideal multilamination is predicted by the Computational Fluid Dynamics calculations of Schönfeld et al.[16] The range of this laminar regime is also quite close to the one found by Li et al.[9] for Sulzer SMX static mixers at macroscale where the laminar regime exists for $Re < 15$.

In the laminar regime, the power number in a stirred tank $N_p = P/\rho N^3 D^5$ (P is the power, N the rotation speed, and D the diameter of the impeller[25]) is related to the Reynolds number by the following relationship

$$N_p=\frac{K_{p\ impeller}}{Re} \tag{7}$$

$K_{p\ \mathrm{impeller}}$, the power constant is specific to an impeller but does not depend on whether the fluid is Newtonian or non-Newtonian.[26–28]

In analogy with the relationship developed for impellers,[26] a power constant can be defined for micromixers. A generalized relationship of the form $K_p = 4\ f/2\ Re$ can be defined for static mixers or any kind of pipe geometry to relate the pressure drop to the Reynolds number.[11,13] In our case, the value of the power constant is $K_p = 96$. Table 4 compares the pressure drop correlations for different kinds of static mixers. It appears that the pressure drop in the Caterpillar is significantly lower than in the Kenics or SMX static mixers.

Table 3. Viscoelastic Characteristic Time λ_{ve} of the Different PAAm Solutions Obtained by Fitting of the Relative Excess Pressure Drop (Curves Plotted in Figure 8)

	λ_{ve} (s)	b	λ_E (s)
PAAm 0.1%	0.052	0.828	0.08
PAAm 0.25%	0.123	0.85	0.21
PAAm 0.5%	0.099	0.91	0.39

Elongational characteristic times are given in the last column.

Pressure drop in case of shear-thinning or viscoelastic PAAm solutions

The pressure drop for non-Newtonian fluids in static mixers has not been studied very often. The few existing studies[10,13,29] did not consider highly elastic fluids. In our experiments, the friction factor of a shear-thinning Carbopol 940 solution and of highly viscoelastic PAAm solutions was measured over a large range of flow rates (Figure 7). The viscosity of these non-Newtonian fluids is shear thinning

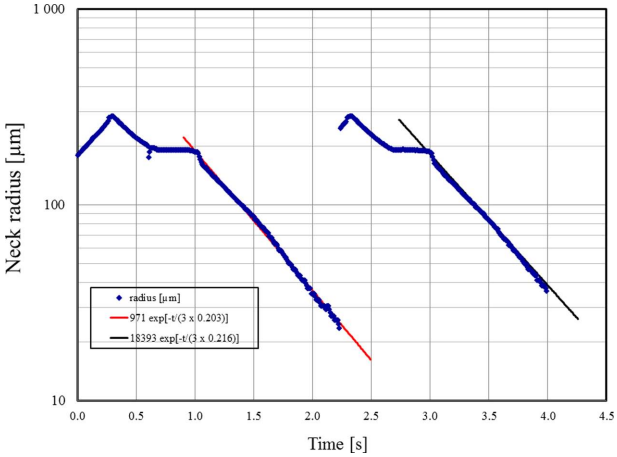

Figure 5. Scaling of the filament thinning for a 0.25% PAAm aqueous solution.

[Color figure can be viewed in the online issue, which is available at wileyonlinelibrary.com.]

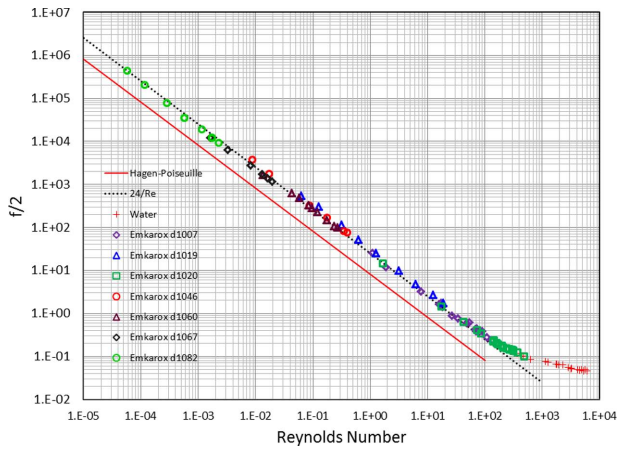

Figure 6. Friction factor for Newtonian fluids: distilled water and Emkarox/water mixtures.

[Color figure can be viewed in the online issue, which is available at wileyonlinelibrary.com.]

Table 4. Power Constant K_p for Different Static Mixers

Geometry	K_p	Reference
Empty tube	32	Hagen–Poiseuille flow
Caterpillar	96	This study
Kenics	170	Chemineer documentation
SMX	1200	Sulzer documentation
SMX	618	Li et al.9

(Figure 3 and Table 2). A generalized Reynolds number based on approximating the shear-thinning behavior of fluids by a power law in a cylindrical pipe is defined as

$$Re_{PL} = \frac{\rho \quad \mathrm{u}^{2-n} d^n}{8^{n-1} k \left(\frac{3n+1}{4n}\right)^n} \tag{8}$$

where k is the consistency and n the flow index.

The friction factor for the Carbopol and PAAm solutions are, respectively, correlated by $f/2 = (27 \pm 1.1)/Re_{PL}$ and $f/2 = (20 \pm 1.05)/Re_{PL}$ for very low Reynolds numbers in the latter case. These correlations are similar to the ones obtained for Newtonian fluids within statistical errors. The measurement of the non-Newtonian viscosities on a rheometer is the main source of uncertainties. They are about the same order of magnitude as the uncertainty on K_p. The Newtonian viscosities were measured on capillary Ubbelohde viscosimeters that have a much higher precision. The shear-thinning Carbopol solution and the viscoelastic shear-thinning solutions of PAAm behave quite differently (Figure 7). The friction factor of the Carbopol solution do not differ significantly from the behavior of the Newtonian fluid, that is, the regime where the friction factor $f/2$ scales as $1/Re_{PL}$ ends up around Re_{PL} values between 10 and 100. The viscoelastic solutions behave completely differently with an increase of the friction factor for $Re_{PL} > 0.01$.

The Metzner–Otto constant K_s[26] is defined as

$$\dot{\gamma}_{eff} = K_s \frac{u}{d} \tag{9}$$

where $\dot{\gamma}_{eff}$ is the effective shear rate of the non-Newtonian fluid going through the Caterpillar. This effective shear rate corresponds to shear rate of a fluid following the same power law and having a process viscosity, η_{PR} corresponding to $K_p = 4f/2\ Re = 96$ for the same velocity u, and same pressure drop ΔP (and, thus, same $f/2$). In naming K_{PNN} the power constant measured for the non-Newtonian fluid

$$\frac{K_{pNN}}{K_p} = \frac{4f/2Re_{PL}}{4f/2Re_{Pr}} = \frac{Re_{PL}}{Re_{Pr}} = \frac{\frac{\rho u^{2-n} d^n}{8^{n-1} k \left(\frac{(3n+1)}{4n}\right)^n}}{\frac{\rho u d}{\eta_{Pr}}} \tag{10}$$

where $\eta_{Pr} = k\left(\dot{\gamma}_{eff}\right)^{n-1} = k\left(K_s \frac{u}{d}\right)^{n-1}$. For the Carbopol 940 solution, $K_s = 5$, whereas for the PAAm solutions, $K_s = 8.5$.

In the case of an emulsification taking place in the Caterpillar, this process shear rate gives the effective shear rate applied on the droplets. Hence, it is a way to estimate the shear forces acting on droplet break-up, a key parameter for an understanding of emulsification process.

Excess pressure drop

In the case of the highly viscoelastic solutions of PAAm, the "laminar" regime, or more accurately, the regime where the friction factor $f/2$ scales as $1/Re_{PL}$, ends up at a Reynolds number of $Re_{PL} = 0.01$. Beyond this "laminar" regime, the friction factor coefficient deviates increasingly from $f/2 = 20/Re_{PL}$. The friction factor $f/2$ becomes much larger than that predicted by this scaling law, although the generalized Reynolds number remains so low that we should still be in the creeping regime.

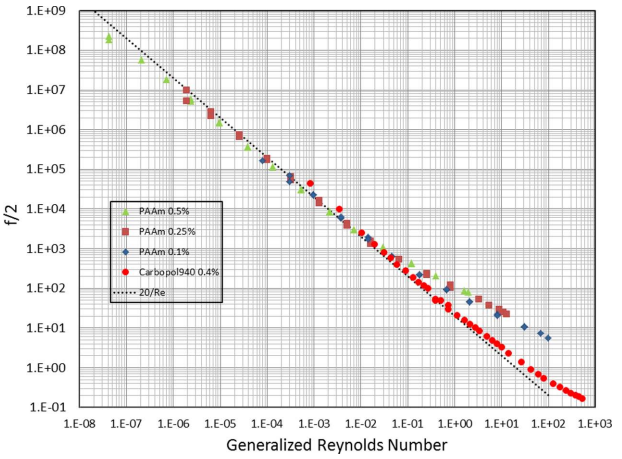

Figure 7. Friction factor for 0.4% shear-thinning Carbopol 940 and viscoelastic fluids: 0.1, 0.25, and 0.5% PAAm aqueous solutions.

[Color figure can be viewed in the online issue, which is available at wileyonlinelibrary.com.]

To our knowledge, pressure drop has not been measured in static mixers for highly viscoelastic fluids, and as a result, the excess pressure drop has not been observed outside Langer and Werner[30] who briefly mention it. However, this sharp increase of the friction factor with the flow rate has often been observed on flow of viscoelastic fluids in porous media.[23,31,32] Most of the porous media used for these studies were in fact packing beads. The increase in the friction factor in the case of viscoelastic fluids was explained and modeled by an elongation of the fluids going through the successively shrinking and expanding size of the interstice between the beads.[32] The role of the elongational viscosity in the increase of the friction factor has been largely accepted in most of the literature. To prove the validity of this hypothesis, Deiber and Schowalter[33] studied the flow of a viscoelastic fluid in a shaped tube with sinusoidal axial

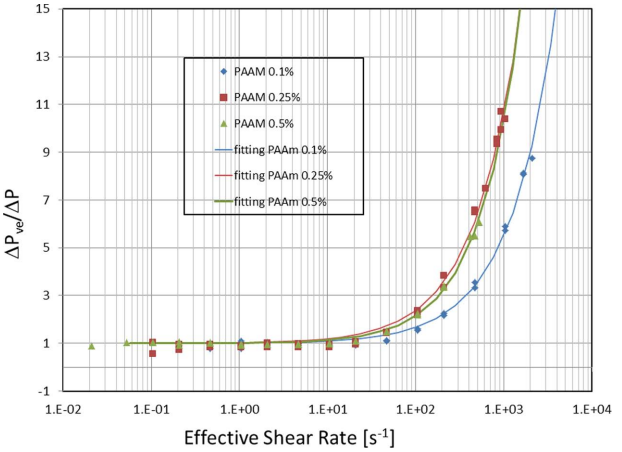

Figure 8. Excess pressure drop measured in case of 0.1, 0.25, and 0.5% PAAm solutions.

[Color figure can be viewed in the online issue, which is available at wileyonlinelibrary.com.]

variation of the diameter. They observed a clear increase in the friction factor and also developed a theoretical model of the flow in this wavy tube, confirming the importance of the elongational flow in the increase of the frictions. Their observations were confirmed by Koshiba et al.[34] in an undulating channel. It is particularly relevant to link the elongation of the fluid to the excess pressure drop, because there is also a kind of successive shrinking and expanding size of the cross section in the Caterpillar.

An interesting way to represent this excess pressure drop is to plot $\Delta P_{ve}/\Delta P$ in function of the effective shear rate $\dot{\gamma}_{eff} = K_s \frac{u}{d}$ (Figure 8). ΔP_{ve} is named "viscoelastic excess pressure drop" and is the actual pressure drop measured for $Re_{PL} > 0.01$. ΔP is the pressure drop that would have been measured if the scaling law obtained for $Re_{PL} < 0.01$ would be extendable to higher Reynolds numbers.

Following Ref. 23, the excess pressure drop can be expressed as a function of a Deborah number $De = \frac{\lambda}{t_p}$, where λ is a fluid characteristic time and t_p is a process characteristic time that is taken here as $t_p = \frac{1}{\dot{\gamma}_{eff}} = \frac{d}{K_s u}$.

The relative excess pressure drop can be fitted by

$$\frac{\Delta P_{ve}}{\Delta P} = f(De) = 1 + \left(\lambda_{ve}/t_p\right)^b \tag{11}$$

where λ_{ve} is an effective viscoelastic characteristic time of the fluid. Values of λ_{ve} and b for the different PAAm solutions are given in Table 3.

In their study of excess pressure drop flowing in a fixed bed of particles, Bendova et al.[23] compare this effective viscoelastic time with commonly used characteristic times. The time scale of the Carreau law (Table 2) is orders of magnitude larger, but the time scale based on elongational flow λ_E measured on a polymeric filament thinning gives satisfactory results.

The main conclusions of this part are that (1) the excess pressure drop is related to the polymer solution's viscosity that is elongation-thickening, (2) the Deborah number based on an extensional characteristic time of the fluid is relevant to express the onset of pressure drop, (3) we also have an indirect confirmation that the split and recombining mechanism of the Caterpillar mixers goes with an intense extensional flow of the fluid. The latter has to be taken into account, for example, when handling molecules sensitive to elongation.

Conclusions

The results of this study show that CPMMs have a friction factor scaling as $f/2 = 24/Re$ for Newtonian fluids. This scaling law is valid up to a Reynolds number of about 100 where the laminar regime ends and the intermediate regime leading to turbulence begins. CPMMs have a low friction factor in comparison to other static mixers at macroscale as the Sulzer SMX or Kenics static mixers. The power constant of the Caterpillar is $K_p = 96$.

In the case of viscoelastic fluids, an excess pressure drop due to the viscoelastic properties of the fluids begins at very low Reynolds numbers. The physical mechanism is the same as the one obtained for porous media or beds of packed beads: a succession of elongation/compression of the viscoelastic fluids flowing through. This excess pressure drop exists for any highly viscoelastic fluids in all the static mixers where elongational flows are important, what is the case of most static mixers. Based on the elongation time scale measured on a rheometer, it will be possible to estimate the critical flow rate above which the pressure loss in the static mixer becomes excessive for an economical use.

Acknowledgments

Parts of the work described has been funded within the 6th Framework Program of the European Commission as part of the Integrated Project IMPULSE (Project No. NMP2-CT-2005–011816). M. Weber and A. Benhara from the Electronic shop and P. Beaurain from the Mechanic Machine shop are acknowledged for their help.

Notation

b = exponent of the correlation between the pressure drop and the Deborah number (Eq. 9)
d = Caterpillar characteristic dimension, m
D = diameter of the impeller, m
De = Deborah number
$f/2$ = friction factor
$h(t)$ = width of the neck of the droplet in formation, m
k = flow consistency index, Pa s^n
K_p = power constant
$K_{p\ impeller}$ = power constant for an impeller
K_s = Metzner–Otto constant
l = length of a mixing element, m
L = length of the Caterpillar, m
m = Carreau law flow index
n = flow index
N = rotation speed, rotation s^{-1}
N_1 = first normal stress difference, Pa
N_p = power number
P = power, kg m^2 s^{-3}
Re = Reynolds number
Re_{PR} = process Reynolds number
Re_{PL} = generalized Reynolds number based on a power law
t = time, s
t_p = process characteristic time, s
u = mean velocity, m s^{-1}

Greek letters

ΔP = pressure drop through the static mixer, Pa
ΔP_{ve} = excess pressure drop, Pa
$\dot{\varepsilon}$ = extensional strain rate, s^{-1}
$\dot{\gamma}$ = shear rate, s^{-1}
$\dot{\gamma}_{eff}$ = effective shear rate, s^{-1}
η = dynamic viscosity, Pa s
η_0 = zero shear rate viscosity, Pa s
η_∞ = infinite shear rate viscosity, Pa s
η_{pr} = process viscosity, Pa s
λ = Carreau law time constant, s
λ_{ve} = viscoelastic characteristic time, s
λ_E = characteristic elongational time, s
τ = shear stress, Pa
ρ = density, kg m^{-3}

Literature Cited

1. Mason BP, Price KE, Steinbacher JL, Bogdan AR, McQuade DT. Greener approaches to organic synthesis using microreactor technology. *Chem Rev*. 2007;107:2300–2318.
2. Hessel V, Hofmann C, Löwe H, Meudt A, Scherer S, Schönfeld F, Werner B. Selectivity gains and energy savings for the industrial phenyl boronic acid process using micromixer/tubular reactors. *Org Process Res Dev*. 2004;8:511–523.
3. Hessel V. Novel process windows—gate to maximizing process intensification via flow chemistry. *Chem Eng Technol*. 2009;32:1655–1681.
4. Bayer T, Himmler K. Mixing and organic chemistry. *Chem Eng Technol*. 2005;28:285–289.
5. Geyer K, Codée JDC, Seeberger PH. Microreactors as tools for synthetic chemists—the chemists' round-bottomed flask of the 21st century?. *Chemistry*. 2006;12:8434–8442.

6. Renken A, Hessel V, Löb P, Miszczuk R, Uerdingen M, Kiwi-Minsker L. Ionic liquid synthesis in a microstructured reactor for process intensification. *Chem Eng Process*. 2007;46:840–845.
7. Rothstock S, Hessel V, Löb P, Werner B. Characterization of a redispersion microreactor by studying its dispersion performance. *Chem Eng Technol*. 2008;31:1124–1129.
8. Yoshida J.-I, Nagaki A, Yamada T. Flash chemistry: fast chemical synthesis by using microreactors. *Chemistry*. 2008;14:7450–7459.
9. Li HZ, Fasol C, Choplin L. Hydrodynamics and heat transfer of rheologically complex fluids in a Sulzer SMX static mixer. *Chem Eng Sci*. 1996;51:1947–1955.
10. Li HZ, Fasol C, Choplin L. Pressure drop of Newtonian and non-Newtonian fluids across a Sulzer SMX static mixer. *Trans IChemE A: Chem Eng Res Des*. 1997;75:792–796.
11. Rauline D, Tanguy PA, Le Blévec JM, Bousquet J. Numerical investigation of the performance of several static mixers. *Can J Chem Eng*. 1998;76:527–535.
12. Fradette L, Tanguy P, Li HZ, Choplin L. Liquid/liquid viscous dispersions with a SMX static mixer. *Trans IChemE A: Chem Eng Res Des*. 2007;85:395–405.
13. Fradette L, Li HZ, Choplin L, Tanguy P. Gas/liquid dispersions with a SMX static mixer in the laminar regime. *Chem Eng Sci*. 2006;61:3506–3518.
14. Liu S, Hrymak AN, Wood PE. Laminar mixing of shear thinning fluids in a SMX static mixer. *Chem Eng Sci*. 2006;61:1753–1759.
15. Hessel V, Löwe H, Schönfeld F. Micromixers—A review on passive and active mixing principles. *Chem Eng Sci*. 2005;60:2479–2501.
16. Schönfeld F, Hessel V, Hofmann C. An optimized split-and-recombine micro-mixer with uniform 'chaotic' mixing. *Lab Chip*. 2004;4:65–69.
17. Tofteberg T, Skolimowski M, Andreassen E, Geschke O. A novel passive micromixer: lamination in a planar channel system. *Microfluid Nanofluid*. 2010;8:209–215.
18. Choe J, Seo JH, Kwon Y, Song KH. Lithium-halogen exchange reaction using microreaction technology. *Chem Eng J*. 2008;135S:S17–S20.
19. Löb P, Hessel V, Hensel A, Simoncelli A. Micromixer based liquid/liquid-dispersion in the context of consumer good production with focus on surfactant vesicle formation. *Chim Oggi/Chem Today*. 2007;25:26–29.
20. Choe J, Song KH, Kim JH, Lee SG, Lee SM, Song KH. Gas/liquid dispersion in a sequential split micromixer. *J Ind Eng Chem*. 2008;14:161–165.
21. Funfschilling D, Debas H, Li HZ, Mason TG. Flow-field dynamics during droplet formation by dripping in hydrodynamic-focusing microfluidics. *Phys Rev E*. 2009;80:015301.
22. Arratia PE, Gollub JP, Durian DJ. Polymeric filament thinning and breakup in microchannels. *Phys Rev E*. 2008;77:036309.
23. Bendova H, Siska B, Machac I. Pressure drop excess in the flow of viscoelastic liquids through fixed beds of particles. *Chem Eng Process: Process Intens*. 2009;48;29–37.
24. Sousa PC, Pinho FT, Oliveira MSN, Alves MA. Efficient microfluidic rectifiers for viscoelastic fluid flow. *J Non-Newtonian Fluid Mech*. 2010;165:652–671.
25. Metzner AB, Feehs, Lopez Ramos H, Otto RE, Tuthill JD. Agitation of viscous Newtonian and non-Newtonian fluids. *AIChE J*. 1961;7:3–9.
26. Metzner AB, Otto RE. Agitation of non-Newtonian fluids. *AIChE J*. 1957;3:3–10.
27. Tanguy PA, Thibault F, Brito De la Fuente E. A new investigation of the Metzner–Otto concept for anchor mixing impellers. *Can J Chem Eng*. 1996;74:222–228.
28. Aubin J, Naude I, Bertrand J, Xuereb C. Blending of Newtonian and shear-thinning fluids in a tank stirred with a helical screw agitator. *Trans IChemE Part A: Chem Eng Res Des*. 2000;78:1105–1114.
29. Kumar G, Upadhyay SN. Pressure drop and mixing behaviour of non-Newtonian fluids in a static mixing unit. *Can J Chem Eng*. 2008;86:684–692.
30. Langer G, Werner U. Viscoelastische Effekte beim "laminaren" statischen Mischen. *Chem Ing Tech*. 1996;3:283–287.
31. Marshall RJ, Metzner AB. Flow of viscoelastic fluids through porous media. *Ind Eng Chem Fundam*. 1967;6:393–400.
32. Haas R, Durst F. Viscoelastic flow of dilute polymer solutions in regular packed beds. *Rheol Acta*. 1982;21:566–571.
33. Deiber JA, Schowalter WR. Modeling the flow of viscoelastic fluids through porous media. *AIChE J*. 1981;27:912–920.
34. Koshiba T, Mori N, Nakamura K, Sugiyama S. Measurement of pressure loss and observation of the flow field in viscoelastic flow through an undulating channel. *J Rheol*. 2000;44:65–78.

Manuscript received Feb. 16, 2012, and revision received Nov. 27, 2012.